Singh and Joshi
Journal of Engineering and Applied Science (2024) 71:144
https://doi.org/10.1186/s44147-024-00476-w

Journal of Engineering and Applied Science

RESEARCH Open Access

Design of Y-shaped tri-band rectangular slot DGS patch antenna at sub-6 GHz frequency range for 5G communication

Ajay Singh[1*] and Sunil Joshi[1]

*Correspondence:
ajays.13790@gmail.com

[1] Department of Electronics and Communication Engineering, CTAE, MPUAT, Udaipur 313001, India

Abstract

This paper presents the design and development of a rectangular slot DGS patch antenna fed by a microstrip line, designed to operate across three distinct frequency bands at 4.0 GHz, 4.9 GHz, and 5.5 GHz for 5G wireless communication applications. The antenna design outlined in this study is implemented on a Fr-4 substrate with dimensions measuring $50.5 \times 41.12 \times 1.5$ mm^3. The antenna gains at three frequency bands are 2.69 dBi, 7.27 dBi, and 11.37 dBi having impedance bandwidths of 9%, 8.9%, and 5.1%, respectively. The attained bandwidths are 356 MHz, 443 MHz, and 287 MHz for the respective frequency bands. The radiation efficiencies of the proposed antenna are 90%, 82%, and 79% of the three respective frequencies. Antenna 1 in this study exhibits single-band behavior, effectively covering the single frequency band which is 5.5 GHz (5.3578–5.9519 GHz) 5G unlicensed band 5-GHz WLAN IEEE 802.11a frequency. On the other hand, Antenna 2 demonstrates dual-band characteristics spanning the S-band 3.7 GHz (3.5619–3.8544 GHz) and C-band range 5.1 GHz (4.8496–5.2008 GHz) suitable for mid-band 5G applications. Antenna 3 proposed antenna exhibits a tri-band functionality within the C-band spectrum. The results highlight multiple-band operation, consistent high gain, high directivity, and favorable directional radiation patterns.

Keywords: High gain, 5G tri-band, DGS, Mobile handsets, Highly directivity

Introduction

In recent times, there has been notable expansion and advancement in mobile application and design, largely attributed to the anticipated emergence of the upcoming 5G mobile network. Despite the ongoing rollout of 4G cellular mobile systems in numerous countries, telecommunication industries and researchers have already initiated work on the 5G system. Motivated by the constant demand for faster network speeds and increased system capacity, many nations, including the United States, China, the European Union, Japan, and South Korea, have undertaken extensive research and development efforts to introduce 5G wireless broadband technology before 2020. Future 5G developments must prioritize user needs, ensuring reliability and high service quality in maintaining network performance, including latency, security, availability, reliability,

energy efficiency, and device affordability. While microstrip antennas offer numerous advantages, they also come with certain limitations. These include losses due to leakage at the open boundary, limited radiated power and bandwidth, low-power handling capabilities, and restricted gain. The most widely used method for creating a multiband antenna involves cutting slots of various shapes, such as triangular, rectangular, T, E, and U shapes, within the patch [1–8]. The rise of wearable sensors and body-centric communication systems has underscored the importance of integrating multiple wireless communication standards into a single personal wireless device. To meet the demands of these communication protocols, there is a need for wearable multiband antennas capable of functioning across different frequency ranges. Specifically, these antennas must cover 5.15–5.825 GHz for WLAN and 5.3578–5.9519 GHz for 5G unlicensed band 5-GHz WLAN IEEE 802.11a [9–11].

Over the past few decades, 5G mobile communication systems have seen substantial advancements and are now in high demand due to their notable benefits, such as low latency, high data rates, and high data capacity. The adoption of high data rates, wide bandwidth, and stable gain, already implemented in many areas, will be significantly influenced by 5G. The 5G New Radio includes frequency bands like n77 (3.3–4.2 GHz), n78 (3.3–3.8 GHz), and n79 (4.4–5.0 GHz) for sub-6 GHz 5G applications [9, 12, 13].

It has been well established that the U-slot patch antenna can offer impedance bandwidths exceeding 30% for air substrate thicknesses around 0.08 λ_o and over 20% for microwave substrates of similar thickness. The U-slot was primarily introduced to enhance bandwidth rather than to introduce band notches. In [14], the authors demonstrate that the U-slot technique can also be utilized for designing patch antennas with dual- and multiband characteristics. In [10], the author presented a novel planar compact slot antenna featuring C-shaped and inverted L-shaped slots designed for multiband WiMAX communication. The utilization of triple-band antennas employing slot configurations such as T-shaped, Y-shaped, and triangular slots has been documented in references [10, 14]. This article demonstrates that the Y-shaped technique can extend to designing patch antennas with tri-band characteristics. This Y-shaped configuration can provide a higher impedance BW of the desired tri-band that belongs to the 5G communication lower sub-6 GHz frequencies band (see Table 1).

A range of antennas has been developed to address this need, including wideband, narrowband, dual-band, ultra-wideband (UWB), and multiband antennas. Among these, multiband antennas hold an advantage over ultra-wideband antennas due to their ability to mitigate electromagnetic interference and pulse distortion. These antennas offer a more favorable solution, allowing the incorporation of multiple communication standards into a compact, cost-effective system with high data rate capabilities. The literature contains various examples of multiband and UWB antennas featuring diverse structures [11, 17, 18].

DGS, known as defected ground structures, are geometrically compact slots incorporated into the ground plane of microwave components such as antennas and filters. These structures consist of either a solitary unit cell (single defect) or multiple periodic arrangements. By incorporating defected ground structure (DGS) onto the ground plane of an antenna, the flow of current is disturbed, resulting in changes to the effective capacitance and inductance of the system. This phenomenon ultimately

Table 1 Comparative analysis of with existing antenna designs in terms of antenna performance matrices like sizes, operating bands, design techniques, and antenna parameters like gain, BW, and efficiency

References	Sizes (mm x mm) and substrate	Operating bands (GHz)	Design techniques	Antenna parameters like S11, gain, BW, efficiency
[1]	8 × 5 Rogers RT5880	25.875 GHz 38.75 GHz 43 GHz 46.25 GHz 48.7 GHz 51.5 GHz 71 GHz 83.5 GHz	Rectangular shape and partial ground plane	Gain = 2.8 dBi, 2.1 dBi, 2.7 dBi, 2.2 dBi, 3.1 dBi, 2.5 dBi, 2.1 dBi, and 2.8 dBi
[2]	30 × 30 Roger RT-Duroid	18 GHz	Circular structure with a ring antenna structure as the parasitic element	Gain = 9.18 dBi, BW = 1307 MHz Efficiency = 91.9%
[3]	19 × 25 Fr-4	2.5 GHz 3.5 GHz 5.5 GHz	Two F-shaped slots of the same size are etched on a rectangular patch and a defected ground plane	Gain = 1.5 dBi, 1.7 dBi and 3.05 dBi Efficiency = 87%, 92%, and 95%
[4]	30.33 × 25.34 Fr-4	5.6 GHz	E-shaped microstrip patch antenna (MSA) with defected ground structure	Gain = 9.94 dBi BW = 1.39 GHz Dir = 10.03 dBi
[5]	35.51 × 43.16 Fr-4	2.5 GHz 5 GHz 7 GHz 8.9 GHz 13.7 GHz 15.3 GHz 17.4 GHz 21.8 GHz	Dual inverted triangle and I-slot configuration	BW = 150 MHz 300 MHz 270 MHz 160 MHz 7410 MHz 1340 MHz
[9]	36 × 37 Fr-4	3.45 GHz 5.9 GHz	Dual-band rectangular microstrip patch antennas with slots with an inset-fed technique and parasitic strip-based antenna techniques used	Gain = 3.83 dBi and 0.537 dBi BW = 160 MHz and 220 MHz
[15]	30 × 35 Rogers R04350B	27.5 GHz 28 GHz 28.5 GHz	4-port (MIMO) antenna array, two identical rectangular-shaped slotted patch arrays excited by the feed network based on a T-junction power combiner/divider	Gain = 8.45 dBi, 8.1 dBi, 8.22 dBi, respectively Efficiency = 80%, 82%, 85%, respectively
[16]	90 × 80 Fr-4	3.67 GHz	The cross-dumbbell-shaped slot is used as DGS on the ground layer	BW = 13.37%

facilitates antenna miniaturization. Numerous research efforts have documented the application of DGS to reduce the size of patch antennas [4, 15, 16, 19, 20]. Defected ground structure (DGS) is an emerging method aimed at enhancing narrow bandwidth, high selectivity, and low gain in microwave circuits [21]. DGS finds applications in antennas [22–24] and various other microwave components. Previous studies [10, 25] have employed circular and rectangular DGS shapes to perturb the electric field on the ground layer [16].

EMI, or electromagnetic interference, arises from the interaction of electrical and magnetic fields. It occurs when the electromagnetic field of one electronic or electrical device disrupts another device's operation. EMI occurs when both electrical and magnetic fields are active. When multiple signals run concurrently, they generate electric and magnetic fields, emitting electromagnetic waves. These waves from one signal can interfere with those of other signals and vice versa [26].

The microstrip patch antenna exhibits limitations such as low gain, narrow bandwidth, and radiation power losses. To address these issues, a solution involving the integration of slot pairs at opposing edges of the rectangular patch was introduced in reference. The patch and ground plane configuration adjustments improved the antenna's bandwidth [27–29].

This research paper introduces a semicircular rectangular slot DGS structure microstrip patch antenna featuring strips slotted DGS geometry used for achieving high gain. This DGS geometry helps to operate the tri-band functionality and enhance the antenna's gain. This antenna design effectively operates across three distinct frequencies, exhibiting high gain across all three frequency bands. Additionally, the antenna maintains a compact size, measuring 50.5×41.21 mm^2.

Proposed antenna design methodology

Figure 1 depicts a tri-band patch antenna featuring a rectangular slot defected ground structure (DGS) arrangement. The 26.5 mm × 10 mm rectangular slot is positioned on the top of the patch along the *y*-axis. Notably, one end of the rectangular slot is open, while the other end is enclosed within the antenna's patch. This configuration utilizes Fr-4 as the dielectric substrate, having a permittivity of 4.4 and a thickness of 1.5 mm. FR-4 is used in 5G antenna design mainly due to its cost-effectiveness, mechanical strength, thermal stability, and sufficient electrical performance for numerous 5G applications, particularly within the sub-6 GHz frequency range. The antenna is designed for triple-band operation within the C-frequency range and employs a 50 Ω microstrip feed setup along with a rectangular slot. The FR4 dielectric substrate's dimensions measure 50.5 mm in width and 41.21 mm in length, while the height (h) is set at 1.5 mm.

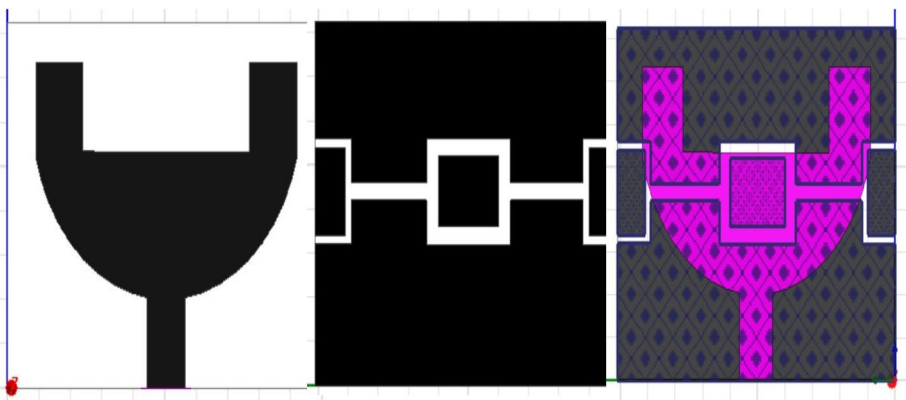

Fig. 1 Illustrating the designed antenna in parts. **a** Top radiating sight. **b** Defective ground sight. **c** 3D representation

The antenna's configuration involves arranging semi-circular rectangular radiating elements horizontally in a scoop-like pattern on the upper surface of the Fr-4 substrate material. The lower surface features a rectangular DGS ground plane.

For impedance matching, a 50 Ω strip lines measuring 6 mm × 11 mm is integrated into the design. To achieve tri-frequency bands, a DGS geometry is introduced. This DGS geometry encompasses a central rectangle situated at the ground plane's center, complemented by two half rectangles positioned at the edges along the *X*-axis. The antenna's patch has dimensions of 41.5 mm × 26.71 mm, and it is excited through a microstrip feed line measuring 6 mm × 10 mm.

Figure 2a, b, and c illustrates the progressive development of the antenna design to get tri-band functionality for 5G communication applications. The diagram showcases the evolutionary steps taken in the antenna's design process to enable it to operate across three distinct frequency bands. As the design progresses, it undergoes modifications and enhancements to cater to the specific requirements of 5G and WLAN and

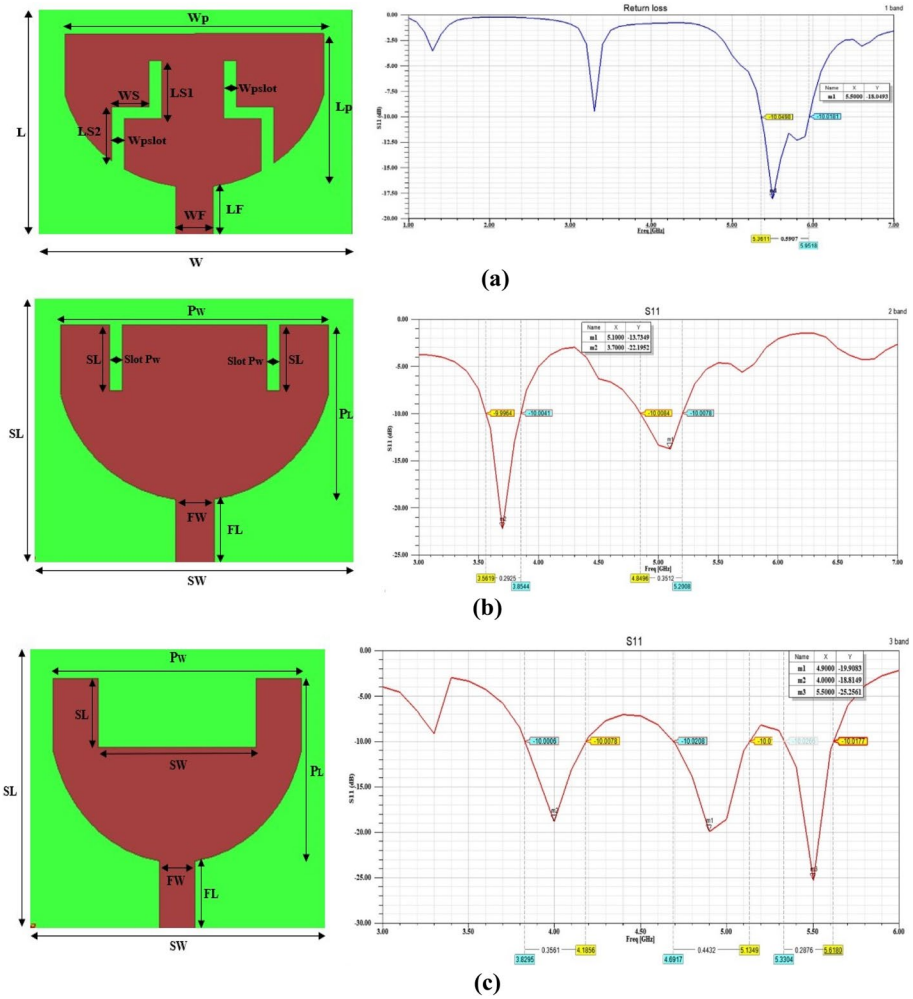

Fig. 2 Antenna evolution progress with reflection coefficient. **a** Iteration slot patch antenna (Antenna 1). **b** Two-rectangular strip slot patch antenna (Antenna 2). **c** Rectangular slot patch (Antenna 3) studies of the proposed antenna

WiMAX communication standards. The ultimate goal is to create an antenna that can efficiently and effectively transmit and receive signals in all three frequency bands, thereby offering seamless connectivity for both WLAN, WiMAX, and 5G communication applications.

The design procedure and prototype of the proposed antenna are visually explained in Fig. 2a, b, and c. In Fig. 2a, the initial design involves a single-band antenna with dimensions of 50.5 mm × 41.21 mm × 1.5 mm, as presented in this configuration "Antenna 1". This antenna is referred to as the "iteration slot patch antenna". In this geometry, an iteration strip slot is introduced on the patch of the antenna, resulting in the antenna being resonant at a single frequency band of 5.5 GHz. By introducing these iteration slots, the total current path length is increased, leading to a disturbance in the surface current distribution of "Antenna 1". As a consequence of these changes, the proposed antenna resonates at 5.5 GHz.

Antenna 2 in Fig. 2b demonstrates that it has achieved resonances at two different frequencies 3.7 GHz and 5.1 GHz. These resonances are made possible by modifying the radiating patch of the antenna. The modification involves the two strip slots inserted on the open side of the radiating patch. The dimensions of the strip slots are 2 mm × 10 mm. These slots play a crucial role in enabling the antenna to resonate at the specified frequencies, allowing it to operate effectively in both the 3.7 GHz and 5.1 GHz bands. This design enhancement enables the antenna to support multiple frequency bands, making it suitable for 5G smartphones, and WLAN/WiMAX applications that require operation across different frequency ranges.

In Antenna 3, a rectangular slot is introduced, leading to significant improvements in its performance. As a result of this change, the antenna becomes capable of operating over three distinct frequencies, which are 4.0 GHz, 4.9 GHz, and 5.5 GHz. In this geometric configuration, a rectangular slot measuring 26.5 mm × 10 mm is introduced on the open side of the patch, aligned with the *Y*-axis.

The dimensions of the substrate and the ground plane geometry are as proposed antenna. The DGS geometry starts with the rectangular slot etched on the ground plane having a dimension of width slot ground (Wsg) which is 14 mm and length slot ground (Lsg) is 8 mm. And the thickness of the strip used to form rectangular slot WgSlot11 is 2 mm. After being etched above the rectangular slot, the two half-rectangular slots are etched centered to the outer arm and connected with the single strip slot to the centered rectangular slot. The half-rectangular slot in DGS plane, Wsg2 width slot ground 2 is 6 mm and Lsg1 is 11 mm and the thickness of the strip is Wgslot1 is 2 mm and Wgslot 2 is 1 mm (Table 2).

Table 2 Measurement specifications of the DGS ground plane of the proposed antenna

Parameters	Wsg Width slot ground	Lsg Length slot ground	Wsg1 Width slot ground 1	Lsg1 Length slot ground 1	Wsg2 Width slot ground 2	WgSlot1 Width ground slot 1	WgSlot2 Width ground slot 2
Dimension (mm)	14	8	12	11	6	2	1

Table 3 Resonant frequency bands for three different versions of antenna geometry

Antennas	Operating frequencies	Impedance bandwidth
Antenna 1	5.5 GHz (5.3578–5.9519 GHz)	594 MHz
Antenna 2	3.7 GHz (3.5619–3.8544 GHz)	292 MHz
	5.1 GHz (4.8496–5.2008 GHz)	351 MHz
Antenna 3	4.0 GHz (3.8295–4.1856 GHz)	356 MHz
	4.9 GHz (4.6917–5.1349 GHz)	443 MHz
	5.5 GHz (5.3304–5.6180 GHz)	287 MHz

Table 3 provides an overview of the resonant frequencies achieved with this modified antenna design. Additionally, Fig. 5 illustrates the 10-dB bandwidths for the three operating bands, which are measured at 356 MHz, 443 MHz, and 287 MHz for the 1st, 2nd, and 3rd frequency bands, respectively.

Incorporating the rectangular slot is a critical improvement that enables the antenna to cover a broader range of frequencies, making it more versatile and suitable for various applications, particularly in 5G smartphones, WLAN, and WiMAX scenarios where multiple frequency bands are utilized.

The visual representation in Fig. 3 illustrates the progressive development of a 5G tri-band proposed antenna that incorporates DGS, specifically of the rectangular slot etched on the semi-half circular rectangular patch. The proposed Antenna configuration, namely a rectangular slot (SW × SL), a radiating patch (Pw × PL), a microstrip feedline (FW × FL), a substrate plane (SW × SL), and a grounding surface (W × L) (Table 4).

At first, an iteration slot patch antenna was formulated using a defective ground structure geometry to function within a sole frequency band at 5.5 GHz. To facilitate two frequency band operations encompassing 3.7 GHz and 5.1 GHz, a two 2 mm × 10 mm rectangular strip slot patch was integrated onto the antenna's

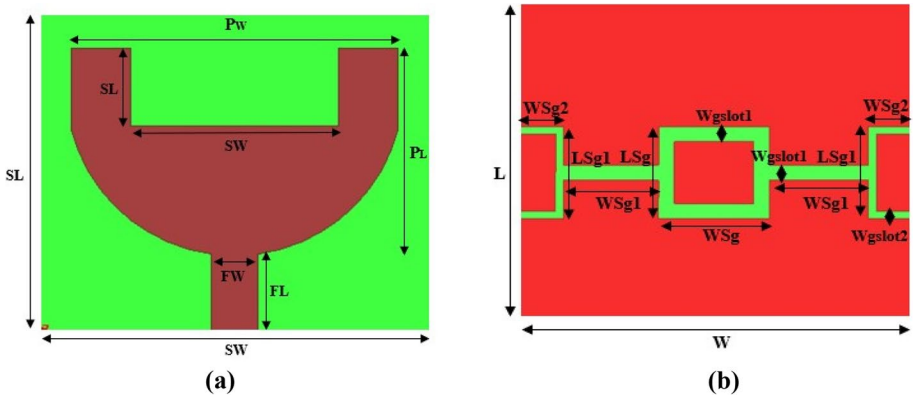

Fig. 3 Proposed antenna structure design. **a** Antenna patch surface. **b** Surface of the grounding plane

Table 4 Measurement specifications of the proposed antenna

Parameters	SW	SL	Pw	PL	FW	FL	SW	SL
Dimension (mm)	50.5	41.21	41.5	26.71	6	10	26.5	10
Parameters	Wsg	Lsg	Wsg1	Lsg1	Wsg2	WgSlot1	WgSlot2	
Dimension (mm)	14	8	12	11	6	2	1	

configuration 2. This Antenna 2 configuration is called a two-rectangular strip slot patch antenna. And the final and proposed configuration was used to cut the rectangular slot positioned at the upper part of the patch. This proposed antenna is named a rectangular slot patch antenna. This modification resulted in an additional operating band; we get the three operating frequencies band 4.0 GHz, 4.9 GHz, and 5.5 GHz.

A tri-band antenna with dimensions $50.5 \times 41.21 \times 1.6$ mm^3 has been developed, as demonstrated in the "Antenna 3" configuration or rectangular slot patch antenna in Fig. 3. This antenna achieves its tri-band functionality by implementing rectangular slots on the top of the radiating patch element. Incorporating this slot extends the overall path that the current follows, causing alterations in the surface current distribution. Consequently, the "Antenna 3" configuration or rectangular slots patch exhibits its resonance at 4.0-, 4.9-, and 5.5-GHz frequencies. These resonant frequencies are visually represented in Fig. 2c.

The proposed antenna is achieved by incorporating defected ground structure (DGS) geometry, as depicted in Fig. 3b. The integration of the DGS structure introduces modifications in the effective inductance and capacitance, resulting in changes to the surface current distribution and input impedance. This adjustment enables a reduction in the size of the antenna while maintaining the desired resonant frequencies. This antenna geometry introduces defected ground structure geometry for achieving high gain and highly directive antenna. DGC geometry consists of a rectangle placed in the center of the ground plane and two half rectangles placed on the *Y*-axis edges of the ground plane. The antenna design consists of semi-circular rectangular radiating elements resembling scoop shape, arranged adjacently on the upper surface of the substrate. On the underside of the substrate, there is a rectangular defected ground plane. The excitation of the radiating element is achieved through a microstrip feed line, which measures 6 mm in width and 11 mm in length. The optimized value of the parameters is illustrated in Table 3. The dimension of the DGS tri-band antenna are determined via the following equations provided below (Fig. 4).

The patch dimensions are acquired using the equations presented below:

$$PW = \frac{c}{2fr\sqrt{(\varepsilon r + 1)/2}} \tag{1}$$

$$PL = \frac{c}{2fr\sqrt{\varepsilon ff}} - 2\Delta L \tag{2}$$

$$\varepsilon ff = \frac{\varepsilon r + 1}{2} + \frac{\varepsilon r - 1}{2}\{1 + 12h/PW\}^{0.5} \tag{3}$$

$$\Delta L = 0.412[(\varepsilon ff + 0.3)(\frac{PW}{h} + 0.264)/(\varepsilon ff - 0.258)(\frac{PW}{h} + 0.8)] \tag{4}$$

Here, "c" symbolizes the velocity of light, "fr" represents the operational frequency, "ΔL" signifies the extension length, and "εff" corresponds to the effective dielectric constant.

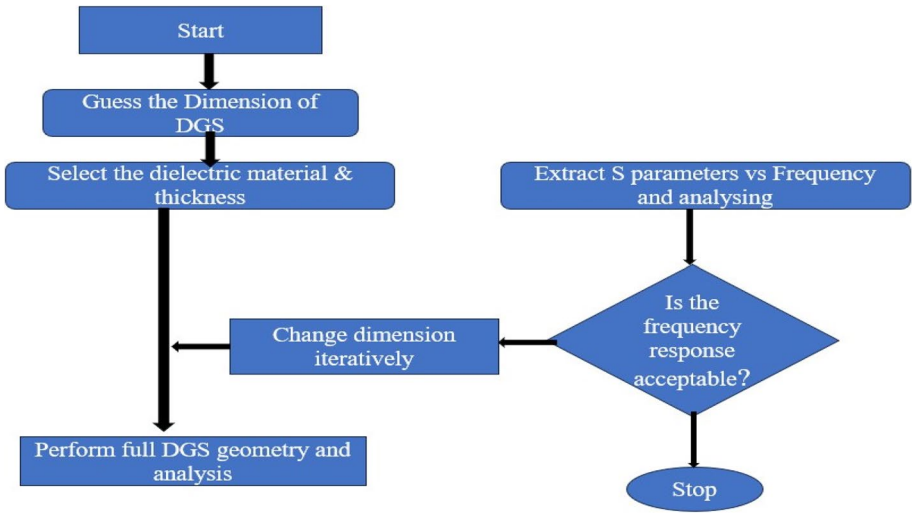

Fig. 4 DGS design optimization process

The dimensions of the ground plane are derived using the equations presented below.

$$GL = 6h + PL \tag{5}$$

$$GW = 6h + PW \tag{6}$$

Here, "h" represents the substrate thickness, "PW" corresponds to the patch width, and "PL" indicates the patch length.

Results and discussion

The S11 characteristics of the tri-band microstrip patch antenna (MPA) demonstrate resonance frequencies at 4.0 GHz, 4.9 GHz, and 5.5 GHz, as illustrated in Fig. 5. The S11 characteristics of the designed antenna cover the frequency ranges of 3.82–4.18 GHz (impedance bandwidth of 356 MHz or 9%), 4.69–5.13 GHz (impedance bandwidth of 443 MHz or 8.9%), and 5.33–5.61 GHz (impedance bandwidth of 287 MHz or 5.1%), centered at frequencies of 4 GHz, 4.9 GHz, and 5.5 GHz, respectively.

$$\%\, Impedance\, Bw = \frac{F_H - F_L}{\frac{F_H + F_L}{2}} \times 100$$

The simulated VSWR plotted against frequency for the proposed antenna consistently showed values lower than 1.5 at the designated operating frequencies, as depicted in Fig. 6. This observation signifies that the designed antenna is well-suited for utilization across the three intended frequency bands. VSWR serves as a metric for assessing the degree of impedance mismatch between the antenna and the feeding system. Higher VSWR values correspond to increased mismatch. A VSWR of 1 indicates a perfect match, while VSWR values greater than 2 indicate a level of mismatch. The VSWR is quantified as the ratio between the maximum and minimum voltages along the transmission line. Figure 5 illustrates the VSWR values for the designed antenna, indicating

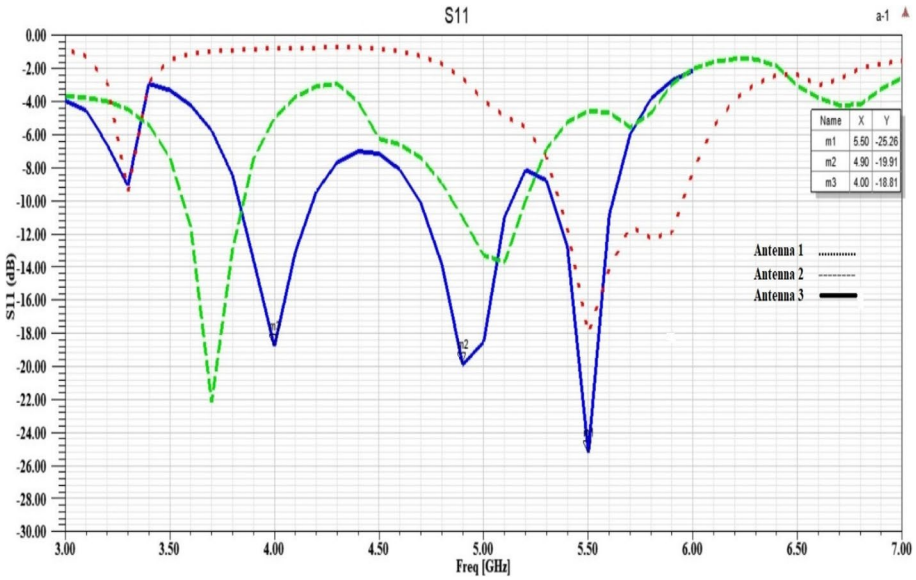

Fig. 5 Simulated reflection coefficient of the proposed antenna

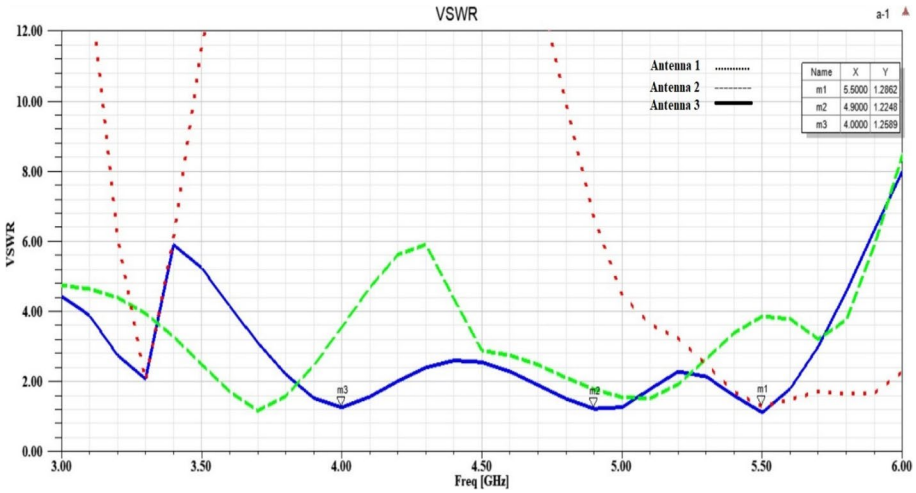

Fig. 6 Depicts the VSWR plot for the tri-band antenna

VSWR values of 1.25 at the 4.0-GHz frequency band, 1.22 at the 4.9-GHz frequency band, and 1.28 at the 5.5-GHz frequency band.

From Fig. 7, the simulated gain for the tri-band antenna is documented as 2.69 dB, 7.26 dB, and 11.36 dB at the respective frequency bands of 4.0 GHz, 4.9 GHz, and 5.5 GHz. Directivity measures the extent of power concentration in a specific direction relative to the power distribution across all directions. Figure 8 illustrates the directivity graph of the antenna design at three distinct operational frequencies: 4.0 GHz, 4.9 GHz, and 5.5 GHz. The depicted values for directivity are 3.17 dBi, 8.13 dBi, and 12.39 dBi for the respective frequencies.

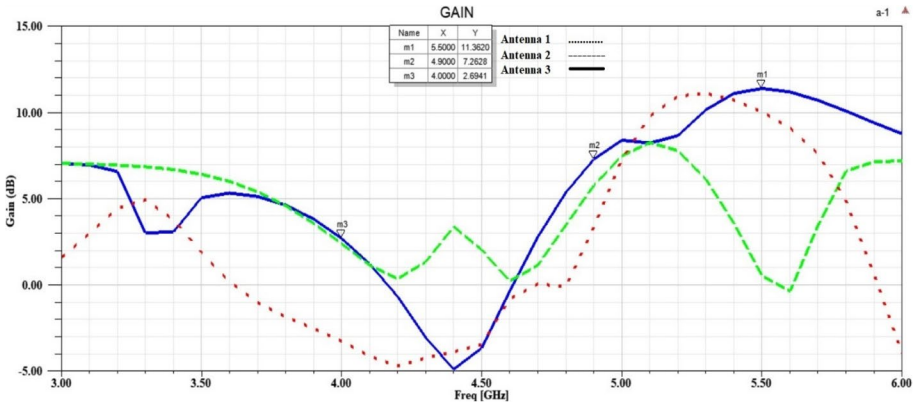

Fig. 7 Gain (dB) of the tri-band antenna

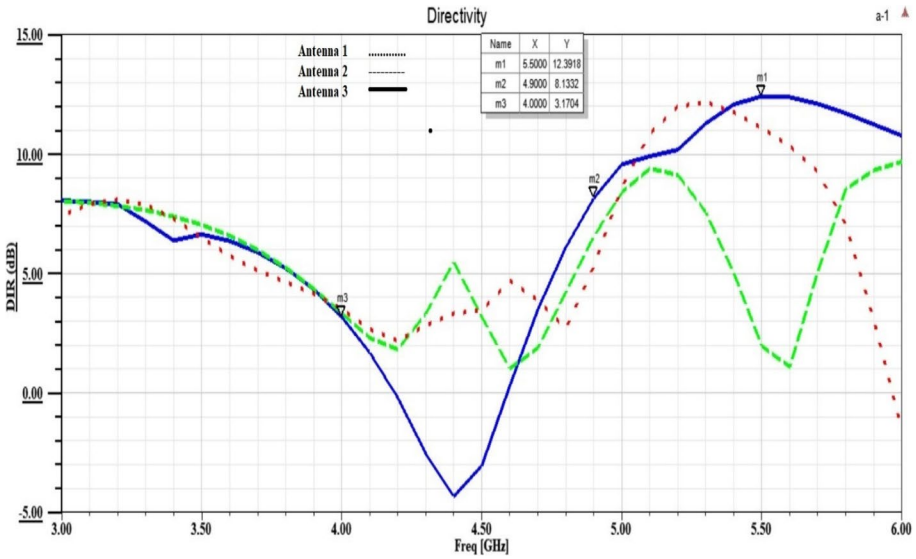

Fig. 8 Directivity (dBi) of the proposed antenna

The radiation efficiency is a crucial factor in assessing the performance of the microstrip patch antenna as it is inversely related to radiation losses. A higher radiation efficiency is preferred for improved suitability to users, with values ranging from 0 to 100%. The CST software is used to compute the total efficiency of the proposed design concerning Antenna 1, Antenna 2, and Antenna 3. Figure 9 presents the simulated radiation efficiency values of the designed antenna. The simulation results reveal that the antenna's radiation efficiency consistently exceeds 78% across the entire operational bandwidth. The highest radiation efficiency was achieved 90% at 4.0 GHz, 82% at 4.9 GHz, and 79% at 5.5-GHz operating frequencies, which is more than that of those presented monopole antenna designs [9, 11, 30, 31].

Figure 10 displays the radiation pattern of the tri-band antenna at frequencies of 4.0 GHz, 4.9 GHz, and 5.5 GHz. It portrays patterns in both the E-field (azimuthal plane) and the H-field (elevation plane). At these frequencies, the most pronounced radiation pattern occurs when theta is at 0° in both planes. This pattern is

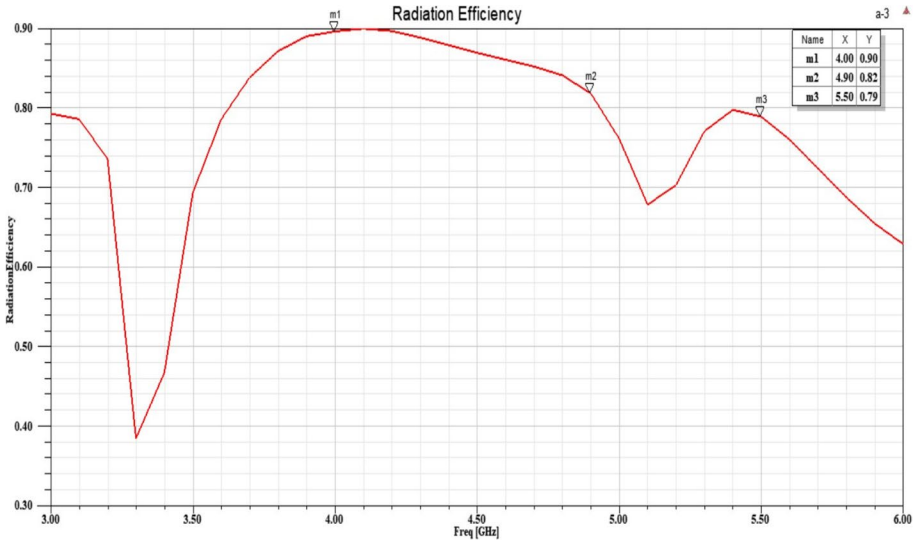

Fig. 9 Radiation efficiency of the proposed antenna

symmetrically replicated in the H-plane. The radiation pattern graph underscores the nearly omnidirectional radiation traits of the tri-band antenna in both the E and H fields (Tables 5 and 6).

Measured results

The reflection coefficient of the fabricated antenna was simulated using Computer Simulation Tools (CST) Microwave Studio (MWS) and measured with a vector network analyzer (VNA). Figure 11a, b, and c illustrate the measurement setup for the proposed Antenna 3. Figure 12 presents the reflection coefficient plot for measured results. For Antenna 3, the |S11| value at the desired frequency ranges was below −10 dB, resonating at 4.0 GHz with a bandwidth of 356 MHz (from 3.8295 to 4.1856 GHz) (n77) and also resonating at 4.9 GHz with a bandwidth of 443 MHz (from 4.6917 to 5.1349 GHz) (n79). Additionally, it achieved a bandwidth of 287 MHz (from 5.3304 to 5.6180 GHz) while resonating at 5.5 GHz. In contrast, the measured results for the n77 (3.3–4.2 GHz) and n79 (4.4 GHz–5.0 GHz) bands showed that the antenna operated at 4 GHz with a bandwidth of 326 MHz (from 3.681 to 4.007 GHz) and at 4.87 GHz, covering a range from 4.539 to 4.982 GHz (443 MHz) for the n79 band.

Conclusions

A tri-band 5G rectangular slot strip DGS patch antenna, incorporating rectangular slot and strip slotted DGS geometry, has been developed, simulated, and evaluated for operation across three distinct frequency bands: 4.0 GHz, 4.9 GHz, and 5.5 GHz. This multiband patch antenna (MPA) is simulated using an FR-4 substrate material with dimensions of 50.5 mm × 41.21 mm × 1.5 mm. The antenna design demonstrates favorable performance attributes, including a notable gain of 2.69 dB, 7.27 dB, and 11.37 dB and a directivity of 3.17, 8.14, and 12.39 dBi at the designated operating frequency of 4.0 GHz, 4.9 GHz, and 5.5 GHz. The reported antenna's radiation

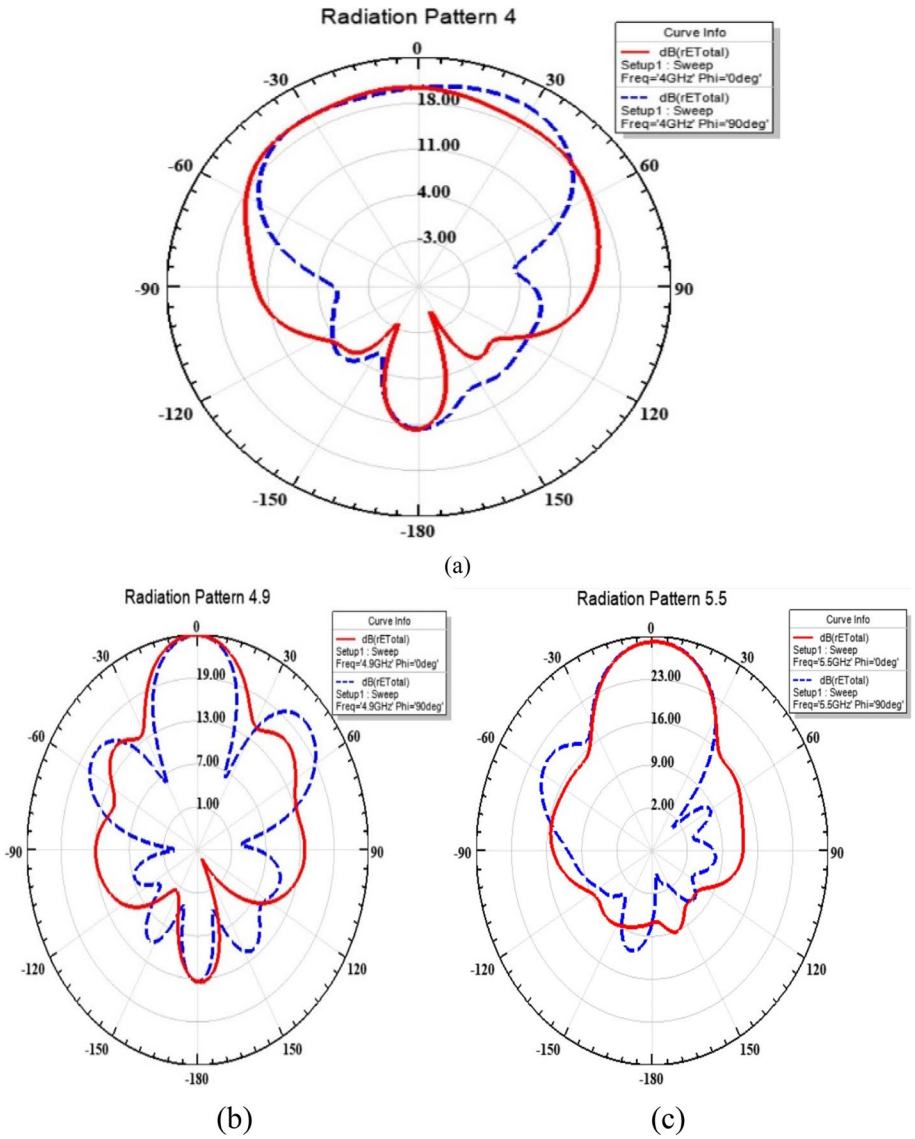

Fig. 10 Illustrating the radiation pattern in both the E-Field and H-field at **a** 4.0-GHz, **b** 4.9-GHz, and **c** 5.5-GHz frequency bands

Table 5 A concise overview of simulated outcomes of Antenna 1, Antenna 2, and Antenna 3

Parameters	Iteration slot patch (Antenna 1)	Two rectangular strip slot patch (Antenna 2)		Rectangular slot patch (Antenna 3) (proposed antenna)		
Operating frequencies	F1 = 5.5 GHz	F1 = 3.7 GHz	F2 = 5.1 GHz	F1 = 4.0 GHz	F2 = 4.9 GHz	F3 = 5.5 GHz
S11 (dB)	−18.05	−22.19	−13.74	−18.82	−19.91	−25.25
VSWR	1.28	1.16	1.51	1.25	1.22	1.11
Gain (dB)	9.99	5.37	8.22	2.69	7.27	11.37
Directivity (dBi)	11.05	5.97	9.36	3.17	8.14	12.39
Radiation efficiency (%)	78%	87%	76%	90%	82%	79%
Impedance BW (MHz)	590	292	351	356	443	287

Table 6 Comparison of proposed work with previous related works

Reference	Operating frequency (GHz)	Impedance BW (MHz)/(% BW)	Gain (dB)	Directivity (dBi)	Radiation efficiency (%)	S11 (dB)
[30]	1.8	320 MHz	4.91		92.45	
	2.4	60 MHz	7.84		75.22	
	3.6	80 MHz	2.58		63.26	
	5.5	180 MHz	4.12		88.95	
[9]	3.45	160 MHz	3.83	5.93	59	−19.36
	5.9	220 MHz	0537	2.75	45	−22.9
[29]	5.38	610 MHz	2.42			−30.88
	6.76	900 MHz	2.46			−45.32
	8.82	910 MHz	4.28			−47.93
[11]	1.5	19.7%	3.01		91	−19
	3.5	5.68%	2.56		85.5	−21.02
	5.2	3.72%	2.92		87	−18.6
	5.8	6.95%	3.9		86	−28.15
[31]	0.82	9 MHz	2.26		36.78	
	1.7	23 MHz	3.42		41.56	
	2.3	34 MHz	2.84		38.15	
Proposed antenna	4.0	356 MHz	2.69	3.17	90	−18.82
	4.9	443 MHz	7.27	8.14	82	−19.91
	5.5	287 MHz	11.37	12.39	79	−25.25

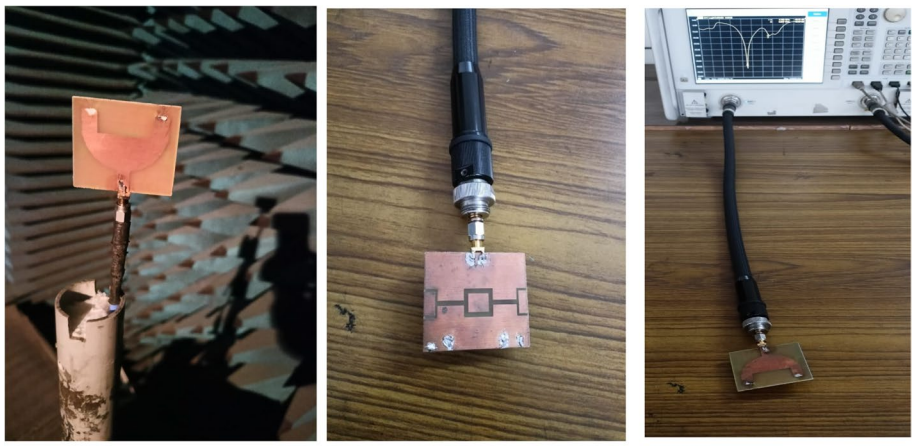

(a) **(b)** **(c)**

Fig. 11 **a** Fabricated measured top radiating sight. **b** Fabricated measured defective ground sight. **c** Measured S11 graph

efficiencies achieve 90%, 82%, and 79% at the respective central frequency, indicating efficient utilization of input power for radiation.

In summary, the introduced microstrip patch antenna incorporating two-strip slotted DGS showcases considerable potential, rendering it well-suited for applications in the realm of 5G and IoT. Notably, it proves advantageous within the LTE band 46 frequencies. With its effective radiation, substantial gain, and omnidirectional

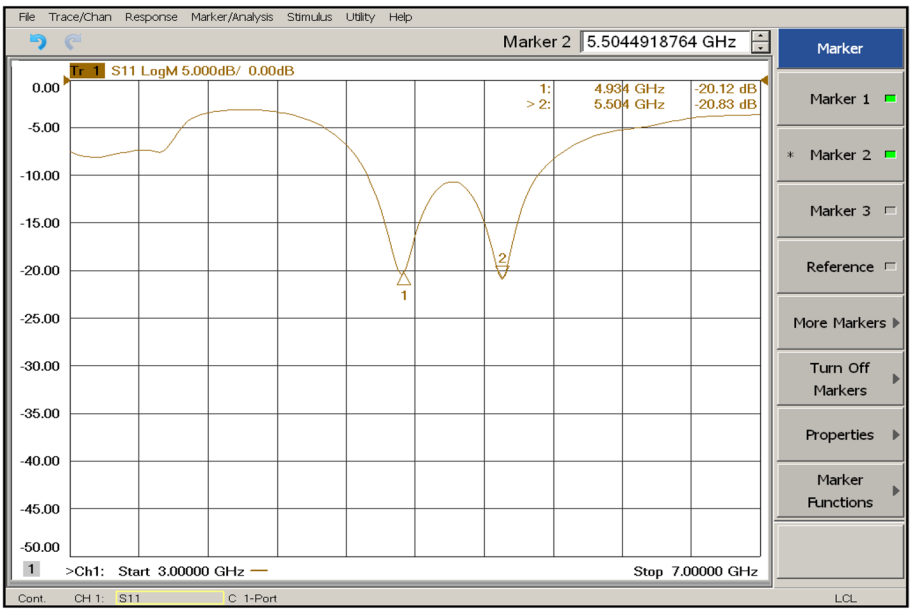

Fig. 12 Measured Reflection coefficient result

radiation pattern, the antenna holds promise as a viable option for diverse 5G communication systems across various scenarios. This proposed antenna is useful for 5G handheld devices. Integrating novel circuitry with antennas is essential to address the demand for active beamforming antenna arrays in 5G telecommunications, particularly within the sub-6 GHz (FR1) frequency range. Future research is necessary to enhance antenna performance by transitioning from a single-element antenna to an array antenna. Antenna arrays with heightened directivity are deployed for fixed-beam communication in the lower sub-6 GHz frequency bands.

Abbreviations

DGS	Defected ground structures
WLAN	Wireless local area network
UWB	Ultra-wideband
IoT	Internet of Things
LTE	Long-term evolution

Acknowledgements
I would like to sincerely thank All India Council for Technical Education (AICTE) for sponsoring a project titled Design and Development of MIMO Antenna for Massive MIMO Array in Shared Spectrum Scenario under RPS (File no. 8-84/FDC/RPS(POLICY-1)).

Authors' contributions
AS, prepared the manuscript and framed the methodology. Dr. SJ, reviewed the manuscript and suggestions for writing the framework of the methodology. Both authors have read and approved the manuscript for submission.

Funding
Not applicable.

Availability of data and materials
Not applicable for this research.

Declarations

Competing interests
The authors declare that they have no competing interests.

Received: 31 August 2023 Accepted: 19 June 2024
Published online: 03 July 2024

References

1. Aziz MAA, Seman N, Chua TH (2019) Microstrip antenna design with partial ground at frequencies above 20 GHz for 5G telecommunication systems. Indones J Electr Eng Comput Sci 15(3):1466–1473
2. Yon H, Abd Rahman NH, Aris MA, Jumaat H (2020) Developed high gain microstrip antenna-like microphone structure for 5G application. Int J Electr Comput Eng 10(3):3086–3094
3. Gautam AK, Kumar L, Kanaujia BK, Rambabu K (2015) Design of compact F-shaped slot triple-band antenna for WLAN/WiMAX applications. IEEE Trans Antennas Propag 64(3):1101–1105
4. Singh A, Joshi S, Dashora D, Lohar L, Paliwal HP (2022) Design and analysis of E-shaped microstrip patch antenna with defected ground structure for improvement of gain and bandwidth. In: Optical and wireless technologies: proceedings of OWT 2020. Springer Singapore, p 195–202
5. Singh A, Joshi S (2023) Design of dual inverted triangular 5G microstrip patch antenna for multiband frequencies. Eur Chem Bull 12(Special Issue 7):7268–7278
6. Kumar M, Saxena R, Ansari JA, Singh A, Siddiqui MG, Saroj AK, Singh GP (2018) Analysis of Half Circular F Slot Multiband Microstrip Antenna with Defected Ground Structure. Recent Advances on Engineering, Technology and Computational Sciences (RAETCS). IEEE, p 1–5
7. Singh A, Singh GP, Manvendra PPC, Kumar M, Saxena R (2017) Analysis of V slot multiband microstrip patch antenna for S, C and X bands. Int J Eng Trends Technol 48:331–334
8. Elkorany AS, Mousa AN, Ahmad S, Saleeb DA, Ghaffar A, Soruri M et al (2022) Implementation of a miniaturized planar tri-band microstrip patch antenna for wireless sensors in mobile applications. Sensors 22(2):667
9. Noor SK, Jusoh M, Sabapathy T, Rambe AH, Vettikalladi H, Albishi AM, Himdi M (2023) A patch antenna with enhanced gain and bandwidth for sub-6 GHz and sub-7 GHz 5G wireless applications. Electronics 12(12):2555
10. Lu JH, Huang BJ (2013) Planar compact slot antenna with multi-band operation for IEEE 802.16m application. IEEE Trans Antennas Propag 61(3):1411–1414
11. Ali T, Biradar RC (2017) A miniaturized Volkswagen logo UWB antenna with slotted ground structure and metamaterial for GPS, WiMAX and WLAN applications. Prog Electromagn Res C 72:29–41
12. Yousif BB, Elsayed EE, Alzalabani MM (2019) Atmospheric turbulence mitigation using spatial mode multiplexing and modified pulse position modulation in hybrid RF/FSO orbital-angular-momentum multiplexed based on MIMO wireless communications system. Opt Commun 436:197–208. https://doi.org/10.1016/j.optcom.2018.12.034
13. Yousif BB, Elsayed EE (2019) Performance enhancement of an orbital-angular-momentum-multiplexed free-space optical link under atmospheric turbulence effects using spatial-mode multiplexing and hybrid diversity based on adaptive MIMO equalization. IEEE Access 7:84401–84412
14. Lee KF, Yang SLS, Kishk AA (2008) Dual- and multiband U-slot patch antennas. IEEE Antennas Wirel Propag Lett 7:645–647
15. Khalid M, Iffat Naqvi S, Hussain N, Rahman M, Fawad, Mirjavadi SS, Amin Y (2020) 4-port MIMO antenna with defected ground structure for 5G millimeter wave applications. Electronics 9(1):71
16. Astuti DW, Fadilah R, Muslim DR, Rusdiyanto D, Alam S, Wahyu Y (2022) Bandwidth enhancement of bow-tie microstrip patch antenna using defected ground structure for 5G. J Commun 17(12):995–1002
17. Dang L, Lei ZY, Xie YJ, Ning GL, Fan J (2010) A compact microstrip slot triple-band antenna for WLAN/WiMAX applications. IEEE Antennas Wirel Propag Lett 9:1178–1181
18. Elsayed EE (2024) Atmospheric turbulence mitigation of MIMO-RF/FSO DWDM communication systems using advanced diversity multiplexing with hybrid N-SM/OMI M-ary spatial pulse-position modulation schemes. Opt Commun 562:130558
19. Ali T, Biradar RC (2018) A triple-band highly miniaturized antenna for WiMAX/WLAN applications. Microw Opt Technol Lett 60(2):466–471
20. Khandelwal MK, Kanaujia BK, Kumar S (2017) Defected ground structure: fundamentals, analysis, and applications in modern wireless trends. Int J Antennas Propag 2017(1):2018527
21. Khandelwal MK, Kanaujia BK, Kumar S (2017) Defected ground structure: fundamentals, analysis, and applications modern wireless trends. Int J Antennas Propag 2017:1–22
22. Patil P, Goilkar S, Deotale N (2019) Microstrip antenna using the defected ground structure for bandwidth enhancement. In: Proc. 4th IEEE international conference on recent trends on electronics, information, communication and technology. p 1384–1388
23. Rusdiyanto D, Apriono C, Astuti DW, Muslim M (2021) Bandwidth and gain enhancement of microstrip antenna using defected ground structure and horizontal patch gap. Sinergi 25(2):153
24. Firdausi A, Wahyudi IM, Wahyudi D, Alaydrus M (2021) Designing Franklin's microstrip antenna with defected ground structure at mmWave frequency. J Commun 16(12):559–565
25. Tang MC, Shi T, Ziolkowski RW (2015) Planar ultrawideband antennas with improved realized gain performance. IEEE Trans Antennas Propag 64(1):61–69
26. Hossain KA (2023) Study on electromagnetic interference (EMI) and electromagnetic compatibility (EMC): sources and design concept for mitigation of EMI/EMC. Journal of Liberal Arts and Humanities (JLAH) 4(8):68–96
27. Jia YS, Wong KL (2000) Bandwidth enhancement bandwidth enhancement using Z-shaped defected ground structure for a microstrip antenna. IEEE Trans Antennas Propag 48:1149–1152
28. Mondal K, Sarkar PP, Chanda Sarkar D (2019) High gain triple band microstrip patch antenna for WLAN, Bluetooth and 5.8 GHz/ISM band applications. Wireless Pers Commun 109:2121–2131
29. Singh PP, Sharma SK (2021) Design and fabrication of a triple band microstrip antenna for WLAN, satellite tv and radar applications. Prog Electromagn Res C 117:277–289

30. Mandal D, Pattnaik SS (2018) Quad-band wearable slot antenna with low SAR values for 1.8 GHz DCS, 2.4 GHz WLAN and 3.6/5.5 GHz WiMAX applications. Prog Electromagn Res B 81:163–182
31. Goud JR, Rao NVK, Prasad AM (2020) Design of triple band U-slot MIMO antenna for simultaneous uplink and downlink communications. Prog Electromagn Res C 106:271–283

Publisher's Note